2022

Experimental Investigation Of A Thermally Integrated Carnot Battery Using A Reversible Heat Pump/Organic Rankine Cycle: Influence Of System Charge On Performance Of The Reversible Scroll Compressor/Expander And Global Performance

Robin Tassenoy

Olivier Dumont

Vincent Lemort

Michel De Paepe

Steven Lecompte

Experimental Investigation of a Thermally Integrated Carnot Battery Using a Reversible Heat Pump/Organic Rankine Cycle: Influence of System Charge on Performance of the Reversible Scroll Compressor/Expander and Global Performance

Robin TASSENOY[1,2]*, Olivier DUMONT[3], Vincent LEMORT[3], Michel DE PAEPE[1,2], Steven LECOMPTE[1,2]

[1]Department of Electromechanical, Systems and Metal Engineering,
Ghent University, Ghent, Belgium
Robin.Tassenoy@UGent.be, Michel.DePaepe@UGent.be, Steven.Lecompte@UGent.be

[2]FlandersMake@UGent – Core lab EEDT-MP,
Leuven, Belgium

[3]Thermodynamics Laboratory, University of Liège,
Liège, Belgium
olivier.dumont@uliege.be, vincent.lemort@uliege.be

* Corresponding Author

ABSTRACT

Carnot batteries are considered a promising power-heat-power storage technology for mid- and large-scale applications. Recently, the use of dual-purpose thermal machines has been proposed in Carnot batteries. In such a system, a single unit acts as heat pump (HP, compressor operation) during charging or organic Rankine cycle (ORC, expander operation) during discharging. This configuration reduces the investment cost of the technology compared to traditional Carnot batteries using two separate machines. An experimental campaign has been performed on a small-scale (1 kW_{el}) Carnot battery pilot plant using a single scroll compressor/expander. A wide range of operational conditions has been tested in both charging and discharging mode. The influence of the system charge on the obtainable working points in both operation modes has been discussed. It has been found that lower system charges are needed to run the system in HP-mode than in ORC-mode. At these low charges, increasing the charge in HP-mode has a positive influence on the system performance at higher source and sink temperatures. At the higher charges for ORC-mode, increasing the system charge has been found to have a positive effect on the start-up of the system in the studied operation range. Next to the qualitative discussion, the system and scroll machine has been studied quantitatively.

1. INTRODUCTION

The growth of renewable energy requires flexible, low-cost and efficient electricity storage to balance the mismatch between energy supply and demand (Dumont et al., 2020). The commercially available large-scale storage technologies suffer from geographical constraints (such as pumped hydro storage and compressed air energy storage), require fossil fuel streams (like compressed air energy storage) or are characterized by a low lifespan (flow batteries and electrochemical cells). There is thus the need for additional large-scale energy storage technologies which do not suffer the abovementioned drawbacks (Agrygou et al., 2018).

Carnot batteries are a novel electrical energy storage (EES) concept that could potentially fulfill these needs. The storage concept involves three distinct processes. First, electrical energy is converted into heat using a joule heater or heat pump. Secondly, this heat is stored in a thermal storage system (TES). Finally, a heat engine technology is used to convert the heat back to electricity when needed. An overview of the different system alternatives has been composed by Dumont et al. (2020). It has been found that the performance of the system can be improved by integrating waste heat sources in the process (Steinmann et al., 2014; Dumont and Lemort, 2020). Configurations

using Rankine-based cycles are particularly suited for thermal integration because of the low temperature range (Dumont et al., 2021). It has been stressed that thermally integrated systems must absorb a thermal input several times larger than the electric one to reach satisfactory performance, which may limit them to small-scale applications (Frate et al., 2020). The system investment cost is crucial for the final feasibility of these systems. Therefore, the use of dual-purpose thermal machines have been proposed for Rankine-based Carnot batteries (Dumont, 2017). In such a system, a single unit acts as heat pump (HP, compression operation) during charging or organic Rankine Cycle (ORC, expander operation) during discharging.

The reversible heat pump/organic Rankine cycle concept has been proven experimentally by Dumont et al. (2021) using a scroll machine. 62 and 60 steady-state points have been acquired for ORC-mode and HP-mode respectively. This first experimental campaign showed a maximum heat pump coefficient of performance of 14.4 (temperature lift equal to 8 K) and a maximum ORC efficiency of 5% (temperature lift equal to 49 K). The temperature lift has been defined as the absolute value of the difference between the saturation temperatures at condensation and evaporation pressure. Although there is a significant amount of measurement points, the system performance has only been evaluated in a limited temperature range. In ORC-mode, the heat source temperature has been varied between 86 and 82 °C. In HP-mode, the maximum condenser inlet temperature tested was limited to 74°C. The tested ranges show only limited overlap and the information useful for successive charging and discharging of the system is thus not investigated in detail yet.

An alternative reversible heat pump/ORC concept using a reversible screw machine has been presented by Staub et al. (2018). The first experimental results of the corresponding prototype with a designed power consumption of 15 kW_{el} at the HP-compressor and a power generation of 9 kW_{el} at the ORC-expander were recently published (Steger et al., 2021). These experimental results have been obtained without insulation and without the thermal storage system. An auxiliary water cycle is used to impose the desired boundary conditions. The start-up behavior has been investigated in detail. Only the nominal operation points have been shown. Special attention has been given to a discussion of the collector vessel, which balances the amount of working fluid in the processes. Although only a limited amount of experiments has been performed, it has shown that the liquid level in the fluid working fluid collector changes with every change in operation in both modes. A constant liquid level in the fluid collector has been found to be a good indicator for accomplishing a steady state. From the nominal points, it becomes clear that the liquid level in the reservoir is lower during ORC-mode compared to HP-mode. This relationship has not been studied in depth yet however.

This study evaluates the performance of the reversible heat pump/ORC prototype introduced by Dumont et al. (2021) in a wider range of operation temperatures representative for successive charging/discharging of the system. As such, additional insight in the performance of the system in the intended operation range has been acquired. The performance of the compressor/expander has been analyzed in both operation modes and its impact on the charging and discharging efficiency has been analyzed. Based on the observations of Steger et al. (2021), the total charge of the system has been varied to investigate the obtainable operation points and operational reliability of the system for different charges. The influence of the system charge on the obtainable operation points and on the system stability is discussed qualitatively first. Afterwards, a quantitative system analysis is presented.

2. EXPERIMENTAL SETUP

2.1 Lay-out

The sizing and nominal conditions of the system are described extensively in Dumont et al. (2020b). A hydraulic scheme of the setup is shown in Figure 1. The refrigerant loop is indicated in dark blue. It contains a high-pressure (hp) heat exchanger (HEX), a scroll volumetric machine (able to work as compressor or expander), a low-pressure (lp) heat exchanger and two parallel branches with a pump (ORC-operation) and an expansion valve (heat pump operation). The refrigerant rotates clockwise in ORC-mode and counter-clockwise in HP-mode. Refrigerant R1233zd(E) is used. The thermal energy storage loop is indicated in red. It consists of two water storages in order to operate with perfect stratification between the hot and cold zone. A circulator provides the necessary flow in the secondary circuit, while a four-way valve is used to provide counter flow in the hp HEX in both operation modes. The light blue water loop is used to regulate the flow rate and temperature of the water entering the lp heat exchanger. Again, a four way valve is used to provide counter flow in the HEX. This water flow functions as heat sink in ORC-

mode and simulates the waste heat input in HP-mode. For a more elaborate discussion on the different components, the reader is referred to Dumont et al. (2021).

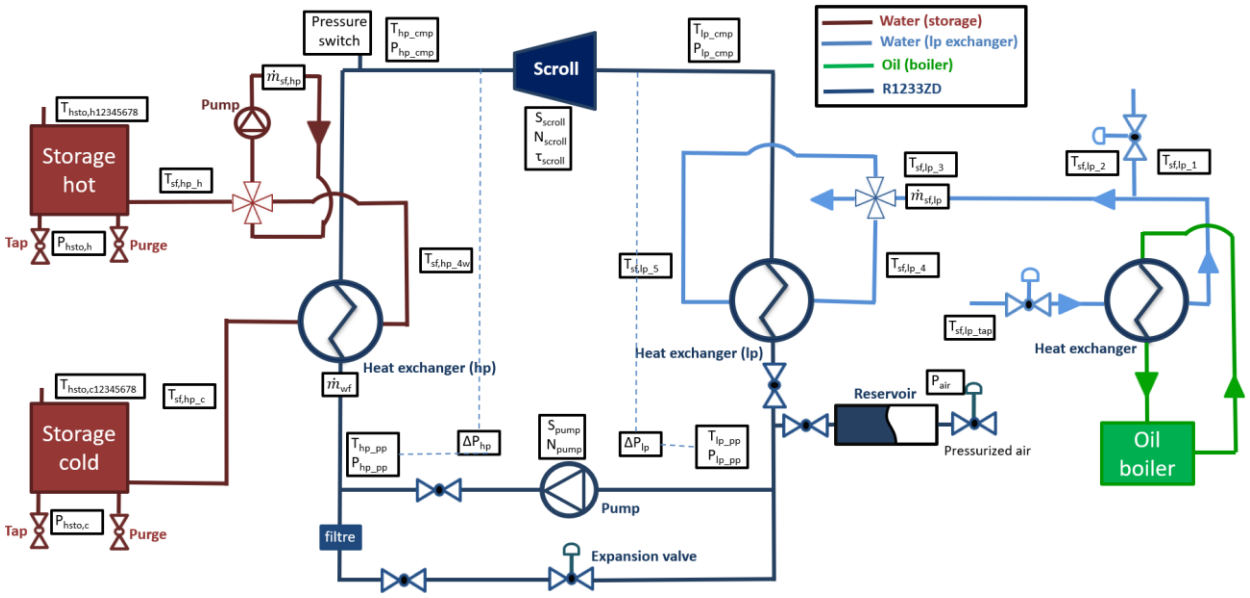

Figure 1: Hydraulic scheme of the Carnot battery test-rig (Dumont et al., 2021).

2.2 Sensors

The test-rig is fully equipped with high accuracy sensors. The measured variables and their location is schematically indicated in Figure 1. An overview of the sensor specifications is provided in Table 1.

Table 1: Technical data of the sensors

Sensor	Parameter	Value
Pressure: Keller PAA23/0-10 bar	Range [bar]	[0-10]
	Maximum pressure [bar]	20
	Accuracy [bar]	0.035
Temperature: Type T	Range [°C]	[-200-200]
	Accuracy [°C]	1
Torque: ETH DRVL-II	Range [Nm]	[0-20]
	Accuracy [Nm]	0.2
Secondary fluid volume flow rate: ROSEMOUNT 8732E	Range [l/s]	[0-1]
	Accuracy [% FS]	0.5
Working fluid mass flow rate: Micro motion F025S	Range [kg/s]	[0.005 – 0.135]
	Accuracy [% FS]	0.2

2.3 Experimental matrix

In total 201 steady-state points have been acquired for HP-mode, while 92 steady-state points have been measured in ORC-mode. The experimental matrices have been defined as function of directly controllable input parameters as much as possible. These parameters include: temperature and volume flow rate of the high-pressure storage loop (ORC: hot reservoir, HP: cold reservoir), temperature and volume flow rate of the low pressure water loop (ORC: heat sink, HP: heat source) and the scroll speed (ORC: expander, HP: compressor). The pump speed (ORC-mode) and valve opening (HP-mode) have been varied depending on the other input parameters in order to get reasonable values for superheating and subcooling. Moreover, the refrigerant charge in the system has been varied in order to assess the influence on the obtainable operational points and corresponding performance. The system charge is expressed relatively to the lowest charge tested. A summary of the directly controlled variable ranges is given in Table 2. A summary of the resulting operational conditions is given in Table 3.

Table 2: input variable ranges

Parameter	**HP**	**ORC**
High pressure reservoir temperature (°C)	[59,0 – 77.4]	[69.9- 82.6]
High pressure volume flow rate (l/s)	[0.30 – 0.49]	[0.27 – 0.42]
Low pressure water temperature (°C)	[29.2 – 62.9]	[14.2 – 37.01]
Low pressure volume flow rate (l/s)	[0.30 – 0.42]	[0.27 – 0.42]
Scroll speed (RPM)	[1000 – 3000]	[1000 – 3000]
Refrigerant charge difference (kg)	[0 – 1.53]	[4.71 – 5.47]

2.4 Performance criteria

The system performance in the different operational points can be characterized by the coefficient of performance (COP) and the global efficiency for heat pump and ORC-mode respectively. The COP and global efficiency can be determined according to Equation (1) and (2). A detailed description of the equation variables and subscripts can be found in the Nomenclature section.

$$COP = \frac{\dot{Q}_{out}}{\dot{W}_{cp,el}} \tag{1}$$

$$\eta_{global} = \frac{\dot{W}_{exp,el} - \dot{W}_{pp,el}}{\dot{Q}_{in}} \tag{2}$$

In which:

$$\dot{Q}_{out} = \dot{m}_r \left(h_{r,cond,su} - h_{r,cond,ex}\right) + \dot{m}_{oil} \left(h_{oil,cond,su} - h_{oil,cond,ex}\right) \tag{3}$$

$$\dot{Q}_{in} = \dot{m}_r \left(h_{r,ev,ex} - h_{r,ev,su}\right) + \dot{m}_{oil} \left(h_{oil,ev,ex} - h_{oil,ev,su}\right) \tag{4}$$

In heat pump mode, the compressor is characterized by the isentropic efficiency (Equation 5) and the volumetric efficiency (Equation 6) (Dumont et al., 2021).

$$\epsilon_{cmp,is} = \frac{\dot{m}_r \left(h_{r,cmp,ex,is} - h_{r,cmp,su}\right) + \dot{V}_{oil}(p_{cmp,ex} - p_{cmp,su})}{\dot{W}_{cp,el}} \tag{5}$$

$$\epsilon_{cmp,vol} = \frac{\dot{V}_{r,cmp,su} + \dot{V}_{oil,cmp,cu}}{\dot{V}_{cmp,th}} \tag{6}$$

In ORC-mode, the expander is characterized by its isentropic efficiency (Equation 7) and its filling factor (Equation 8) (Dumont et al., 2021).

$$\epsilon_{exp,is} = \frac{\dot{W}_{exp,el}}{\dot{m}_r \left(h_{r,exp,su} - h_{r,exp,ex,is}\right) + \dot{V}_{oil}(p_{exp,su} - p_{exp,ex})} \tag{7}$$

$$FF_{exp} = \frac{\dot{V}_{r,exp,su} + \dot{V}_{oil,exp,su}}{\dot{V}_{exp,th}} \tag{8}$$

3. RESULTS AND DISCUSSION

3.1 Operating conditions

Following the experimental matrix, a wide range of operating conditions has been exploited. A summary of these conditions is given in Table 3.

Table 3: Operating conditions

Parameter	HP	ORC
Evaporator thermal power (kW)	[0.598-9.562]	[6.466 – 18.784]
Condenser thermal power (kW)	[0.637-10.434]	[5.953 – 17.188]
Evaporation pressure (bar)	[1.39 – 5.58]	[3.89 – 5.82]
Condensation pressure (bar)	[4.07-7.42]	[1.02 – 3.74]
Mass flow rate (kg/s)	[0.004-0.066]	[0.032 – 0.081]
Subcooling (K)	[0.60 – 3.58]	[7.04-18.01]
Superheating (K)	[1.18 -25.6]	[2.48-5.95]

3.2 Influence of system charge: qualitative discussion

The amount of refrigerant R1233zd(E) in the system has been varied during the experimental campaign. The system charge has been increased gradually. For each charge, it has been attempted to run the setup in all working points of the experimental matrix. The initial system charge was 8.530 kg. The primary results focus on the effect of the charge variation rather than the absolute performance of the proof-of-concept. Therefore, the system charge is expressed as increases in refrigerant charge relative to the initial charge. Following increases have been tested: +0 kg, +0.710 kg, +1.120 kg, +1.530 kg, +4.125 kg, +4.710 kg, +4.965 kg, +5.225 kg and +5.470 kg.

It has been observed that the obtainable operation points depend on the system charge. The charges suitable to run the system in HP- and ORC-mode are different. HP-operation requires lower charges than ORC-operation. For the operational conditions tested, the superheat at the inlet of the compressor decreases with increasing charge. At high charge, this superheating disappears and operation becomes unstable. ORC-mode requires higher system charges however. For the current system, insufficient charge yields too small subcooling at the pump inlet during start-up. Therefore, the pump cannot entrain liquid and no pressure difference can be built up. During the experimental campaign, the system could not be operated reliably in either operation mode for an intermediate charge increment of +4.125 kg. This indicate that the suitable system charge ranges for both modes do not overlap.

Only the four lowest system charges tested are suitable for HP operation. Nevertheless, not all charges were equally suitable for all operation points. A qualitative indication is given in Table 4. From the table, different observations can be made. At the lowest charges, the valve is often fully open especially at low temperature differences between the heat source and sink. As a consequence, the superheating at the compressor outlet is high. This effect is more pronounced at the higher sink temperatures. With increasing charge, the amount of working points where the valve is fully open diminishes. With a further increase in charge, the problem shift to the other end of the experimental matrix. At the highest charges, the valve is almost fully closed in operational points with a large temperature lift. Even with the valve almost closed (and corresponding very low mass flows) the superheating becomes very low and operation becomes unstable.

Table 4: Qualitative suitability of different system charges for HP-mode depending on input parameters and the compressor speed (green: operation OK, orange: operation point difficult, red: impossible to run the system, red letters: valve fully open).

High pressure reservoir T (°C)	Low pressure water T (°C)	Charge: +0 kg	Charge: +0.710 kg	Charge: +1.120 kg	Charge: +1.530 kg
60	56	1000-2000-3000	1000-2000-3000	1000-2000-3000	1000-2000-3000
	51	1000-2000-3000	1000-2000-3000	1000-2000-3000	1000-2000-3000
	45	1000-2000-3000	1000-2000-3000	1000-2000-3000	1000-2000-3000
	38	1000-2000-3000	1000-2000-3000	1000-2000-3000	1000-2000-3000
70	65	1000-2000-3000	1000-2000-3000	1000-2000-3000	1000-2000-3000
	60	1000-2000-3000	1000-2000-3000	1000-2000-3000	1000-2000-3000
	56	1000-2000-3000	1000-2000-3000	1000-2000-3000	1000-2000-3000
	51	1000-2000-3000	1000-2000-3000	1000-2000-3000	1000-2000-3000
76	73	1000-2000-3000	1000-2000-3000	1000-2000-3000	1000-2000-3000

	70	1000-2000-3000	1000-2000-3000	1000-2000-3000	1000-2000-3000
	65	1000-2000-3000	1000-2000-3000	1000-2000-3000	1000-2000-3000
	60	1000-2000-3000	1000-2000-3000	1000-2000-3000	1000-2000-3000

As explained before, only the four highest system charges have been found suitable for ORC-operation. The system cannot start up with lower charges as the pump cannot entrain liquid. The subcooling at the pump inlet is too low to run reliably. The qualitative performance for the four highest charges tested is indicated in Table 5. Increasing the system charge simplifies the start-up of the system. At low charges (e.g. +4.710 kg) multiple attempts were needed to get the system running. Start-up of a cold system (e.g. not used directly before) tends to be easier because of the liquid collected at the pump inlet during the cool-down period before. With slightly higher charge, the system can start up reliably when cold. Still the charge is too low to run reliably when the system is hot as insufficient liquid is accumulated at the pump inlet to start up. In these points, the subcooling at the pump inlet can be increased by increasing the sink temperature, resulting in stable operation for both the cold and hot system. For the two highest charges tested, the system runs stable irrespectively of previous use.

Table 5: Qualitative suitability of different system charges for ORC-mode depending on input parameters (blue: different start-ups needed for cold system; orange: cold system only; green: cold and hot system).

High pressure reservoir T (°C)	**Low pressure water T (°C)**	**Charge: +4.710 kg**	**Charge: +4.965 kg**	**Charge: +5.225 kg**	**Charge: +5.470 kg**
75	20	1000-2000-3000	1000-2000-3000	1000-2000-3000	1000-2000-3000
	40		1000-2000-3000		1000-2000-3000
80	20	1000-2000-3000	1000-2000-3000	1000-2000-3000	1000-2000-3000
	40		1000-2000-3000		1000-2000-3000
85	20	1000-2000-3000	1000-2000-3000	1000-2000-3000	1000-2000-3000
	40		1000-2000-3000		

3.3 HP-mode

The performance of the overall system in heat pump mode is shown by its coefficient of performance in Figure 2. In this figure, the temperature lift is the difference between the saturation temperature at condensation and evaporation pressure respectively. As expected (Dumont et al., 2019), the COP reaches high values for low temperature lifts. For similar temperature lifts, higher COPs are obtained at higher sink temperatures. It is noticeable however that the spread on the measured COPs increases with increasing system charge. For similar lift temperatures, the lowest COPs are measured at low scroll speeds and low sink temperatures. This corresponds with the instable operation points indicated in Table 4.

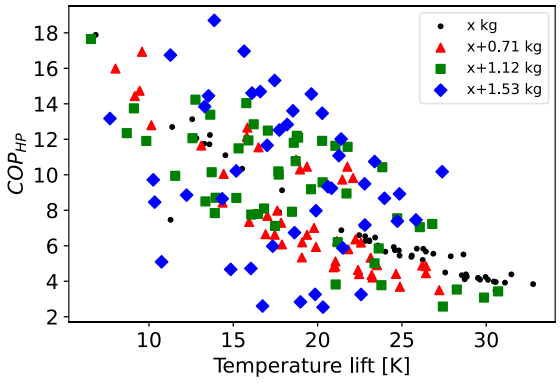

Figure 2: Global performance of the reversible HP/ORC in HP-mode.

In HP-mode, the scroll machine is used in compressor mode. Its performance is presented in terms of mechanical power, isentropic efficiency and volumetric efficiency as function of the scroll speed in Figure 3 for the applicable charges. The corresponding minimum and maximum values of the performance indicators (PI) are listed in Table 6.

The mechanical power of the compressor is shown in Figure 3 (a). The compressor speed has the largest influence on the compressor power. The mechanical power clearly increases with increasing speed. The compressor speed increases with hp reservoir temperature. At constant reservoir temperatures slightly higher mechanical power is observed for lower source temperatures as the pressure ratio slightly increases. These trends are observed for all charges. However, the quantitative values are significantly different for the two lowest (+0 kg, +0.710 kg) and two highest charges (+1.120 kg, +1.530 kg) tested.

The qualitative observations discussed in Table 4 are reflected in the values of the isentropic efficiency (Figure 3(b)). For the experimental matrix, higher system charges result in higher isentropic compressor efficiencies on the whole. However, a clear distinction can be made between the two lowest charges (+0 kg, +0.710 kg) and two highest charges tested (+1.120 kg, +1.530 kg). For the two lowest charges, the isentropic efficiency is the lowest at high temperatures of the hp reservoir and high RPM values. This corresponds to the operation points with a fully open valve and consequently high superheating. For the two highest charges on the other hand, the lowest isentropic efficiencies are calculated for operational points with low hp reservoir temperatures and low RPM values, which corresponds with the instable region with almost closed expansion valve.

The compressor presents a rather constant volumetric efficiency as shown in Figure 3(c) and Table 6. The lower volumetric efficiencies at the highest two charges tested are encountered at low RPM and high lift, especially at low HP reservoir temperatures, which again corresponds with the instable region with almost closed expansion valve. It is noticeable that for the operational conditions tested the volumetric efficiencies are lower than the values reported by Dumont et al. (2021).

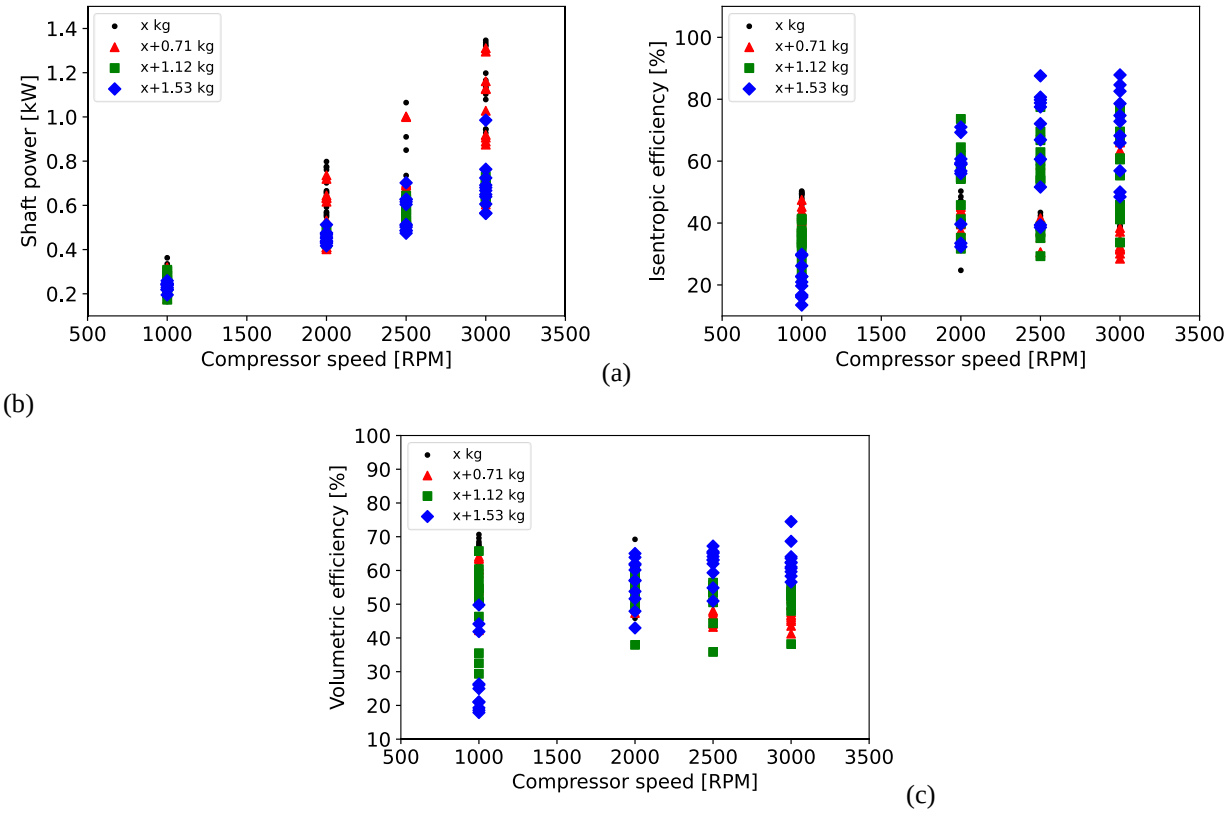

Figure 3: Compressor performance in HP-mode (a) shaft power, (b) isentropic efficiency, (c) volumetric efficiency.

Table 6: Compressor performance in HP mode: minimum and maximum values of PI per system charge.

	Shaft power [kW]		Isentropic efficiency [-]		Volumetric efficiency [-]	
Mass	**Min**	**Max**	**Min**	**Max**	**Min**	**Max**
+0 kg	0.165	1.346	0.25	0.50	0.458	0.706
+0.71 kg	0.177	1.310	0.28	0.69	0.413	0.641
+1.12 kg	0.173	0.730	0.22	0.77	0.293	0.657
+1.53 kg	0.195	0.985	0.14	0.88	0.179	0.745

3.4 ORC-mode

The performance of the overall system in ORC mode is shown through its efficiency in Figure 4. In this figure, the temperature lift is the difference between the saturation temperature at condensation and evaporation pressure respectively. The efficiency is expected to increase with an increasing temperature drop (Dumont et al., 2021). Nevertheless, very high cycle efficiencies are observed at limited temperature drops (or thus high sink temperatures) in Figure 4. These efficiencies are close to or even slightly higher than the corresponding Carnot efficiencies based on the saturation temperatures of the heat exchangers. The torque measured at these high sink temperatures drops only slightly compared to the torque measured at the low sink temperatures. As a consequence, the calculated electrical power is high. Additional verification experiments are needed to clarify these observations or detect potential sensor malfunctions.

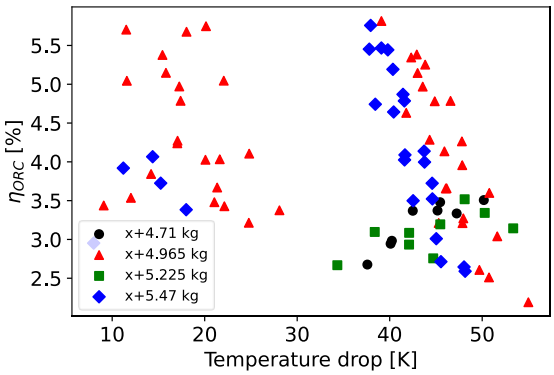

Figure 4: Global performance of the reversible HP/ORC in ORC-mode.

In ORC-mode, the scroll machine is used in expander mode. Its performance is presented in terms of mechanical power, isentropic efficiency and filling factor as function of the scroll speed in Figure 5 for the applicable charges. The corresponding minimum and maximum values of the performance indicators are listed in Table 7.

The expander power is plotted as function of the scroll speed for different charges in Figure 5(a). From the figure, it can be seen that the shaft power increases with increasing scroll speed. Increasing the scroll speed tends to decrease the evaporator pressure. For a given source temperature, higher refrigerant mass flows (and pump speeds) can thus be used (which increases evaporator pressure), while maintaining adequate superheating at the expander inlet. Besides the influence of the scroll speed and refrigerant mass flow, higher source temperatures and lower sink temperatures result in higher shaft power. The minimum shaft power is similar for all charges. The maximum shaft power is significantly different for +4.710 kg and +5.225 kg compared to +4.965 kg and +5.470 kg, despite similar maximum refrigerant mass flows for all charges. The measured torque however shows a different trend. For +4.710 and +5.225 kg charges, the torque measured drops with increasing expander speed. For +4.965 kg and +5.470 kg charges on the other hand the torque stays almost constant for the different speeds. Additional tests have been planned to clarify this behavior or detect potential sensor malfunctions. Within a consistent set of torque measurements, the influence of the system charge on the shaft power is limited.

The evolution of the isentropic efficiency as function of the expander speed is shown in Figure 5(b). The minimum and maximum values per charge are shown in Table 7. Again a difference can be observed comparing the +4.710 kg and +5.225 kg to the +4.965 kg and +5.470 kg charges. For the first set, the isentropic efficiency stays relatively

constant across the conditions tested, while for the latter the isentropic efficiency increases more significantly with increasing RPM. In Figure 5(b) some very high isentropic efficiencies can be observed. These high isentropic efficiencies (some even larger than 100%) correspond to measurements at increased sink temperatures (and thus low temperature drops). The isentropic efficiency is calculated according to Equation (7). The denominator contains the isentropic enthalpy drop corresponding with an idealized isentropic process between the inlet and outlet pressure of the expander. At increased sink temperatures, the expander outlet pressure increases. Consequently, the isentropic enthalpy drop across the expander decreases with 60 to 70 % when the sink temperature increases from 15 to 36 °C. The nominator contains the electrical power (calculated based on the shaft power and thus torque measurement). This electrical power decreases less than 6 % when the sink temperature increases from 15 to 36 °C. The influence of the increasing sink temperature on the nominator is thus smaller than the effect on the denominator, which results in unfeasibly high isentropic efficiencies. This again illustrates the need for additional verification of the torque sensor measurements to justify these quantitative results.

Finally, the filling factor is shown in Figure 5(c). The scroll speed has the most pronounced effect on the filling factor (FF). The expander filling factor decreases with increasing expander speeds, which can be attributed to the lower influence of internal leakages at higher mass flow rates. At a given scroll speed, the FF decreases slightly with increasing source temperature. The influence of the system charge on the FF is limited.

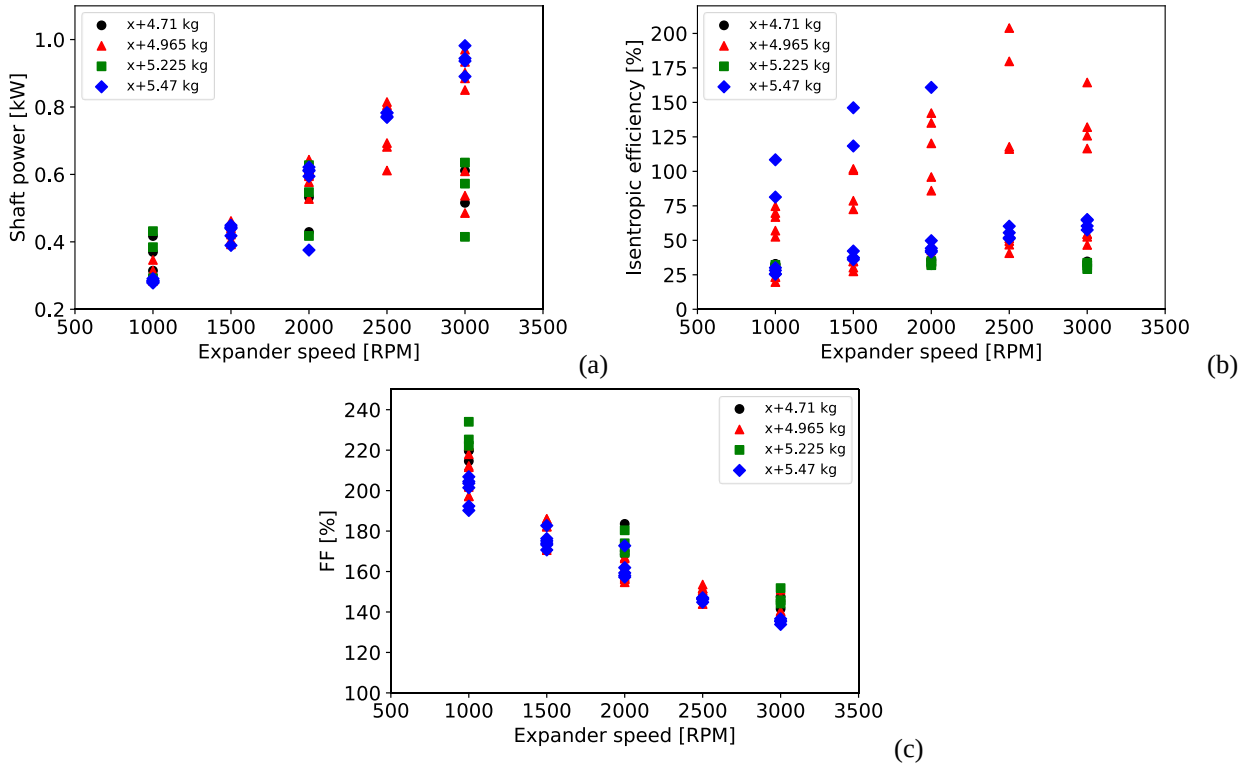

Figure 5: Expander performance in ORC mode (a) shaft power, (b) isentropic efficiency, (c) filling factor.

Table 7: Expander performance in ORC mode: minimum and maximum values of PI per system charge (values between brackets: maximum value at low sink temperature).

	Shaft power [kW]		Isentropic efficiency [-]		Filling factor [-]	
Mass	**Min**	**Max**	**Min**	**Max**	**Min**	**Max**
+4.71 kg	0.315	0.611	0.319	0.358	1.42	2.20
+4.965 kg	0.283	0.970	0.197	2.04 (0.624)	1.36	2.22
+5.225 kg	0.292	0.635	0.280	0.349	1.44	2.34
+5.47 kg	0.278	0.981	0.254	1.608 (0.646)	1.34	2.06

4. CONCLUSION

This paper discusses the experimental results on a proof of concept of a reversible HP/ORC in a wide range of operational conditions. The influence of the system charge on the overall functioning of the system and on the performance of the reversible compressor/expander has been discussed. It has been observed that lower system charges are needed to operate the system in HP-mode compared to ORC-mode. A charge difference of 3.2 kg has been found between the highest mass tested reliably in HP-mode and lowest mass tested reliably in ORC-mode. Within each mode, the specific charge has an influence on the system stability and obtainable operation points. At these low charges, increasing the charge in HP-mode has a positive influence on the system performance at higher source and sink temperatures. At the higher charges for ORC-mode, increasing the system charge has been found to have a positive effect on the start-up of the system in the studied operation range. Currently, the hp and lp volume flow rates have not been varied depending on the operation point. Based on the observations, the use of tank regulation should be explored in future work. Based on this quantitative analysis the influence of different system inputs on the performance is evaluated. While trends are identified, additional verification of the measurement equipment is needed to confirm the obtained numerical values.

NOMENCLATURE

ϵ, η	efficiency	(–)
FF	filling factor	(–)
h	specific enthalpy	(J/kg)
$\dot{m}$	mass flow rate	(kg/s)
$\dot{Q}$	thermal power	(W)
T	temperature	(°C)
$\dot{V}$	volumetric flow rate	(m^3/s)
$\dot{W}$	power	(W)

Acronym

COP	coefficient of performance	(–)
HEX	heat exchanger	(–)
HP	heat pump	(–)
hp	high pressure	(–)
hsto	heat storage	
lp	low pressure	(–)
ORC	organic Rankine cycle	(–)
PI	performance indicator	(–)

Subscript

c	cold
cond	condenser
cmp	compressor
el	electrical
ev	evaporator
ex	exhaust
exp	expander
h	hot
in	input
is	isentropic
oil	oil
out	output
pp	pump
r	refrigerant
sf	secondary fluid
su	supply
th	theoretical

vol volumetric

REFERENCES

Argyrou, M.C., Christodoulides, P. & Kalogirou, S.A. (2018). Energy storage for electricity generation and related processes: Technologies appraisal and grid scale applications. *Renew. Sust. Energ. Rev., 94*, 804–821.

Dumont, O. (2017). Investigation of a heat pump reversible into an organic Rankine cycle and its application in the building sector, PhD Dissertation.

Dumont, O., Frate, G.F., Pillai, A., Lecompte, S., De Paepe, M. & Lemort, V. (2020a). Carnot battery technology: A state-of-the-art review. *Journal of Energy Storage, 32*, 101756.

Dumont, O., Reyes, A. & Lemort, V. (2020b). Modelling of a thermally integrated Carnot battery using a reversible heat pump/organic Rankine cycle. In Yokoyama, R. & Amano, Y. (Eds.), *Proceedings of ECOS2020- The 33rd international conference on Efficiency, Cost, Optimization Simulation and Environmental impact of energy systems, Osaka, Japan* (1412-1422). Osaka, Japan: ECOS2020 Local Organizing Committee

Dumont, O., Charalampidis, A., Lemort, V. & Karellas, S. (2021). Experimental investigation of a thermally integrated Carnot battery using a reversible heat pump/organic Rankine cycle. *18th International Refrigeration and Air Conditioning Conference Proceedings, 2111*, 1-14.

Frate, G.F., Ferrari, L. & Desideri, U. (2020). Rankine Carnot Batteries with the Integration of Thermal Energy Sources: A Review. *Energies 13*, 4766.

Staub, S., Bazan, P., Braimakis, K., Müller, D., Regensburger, C., Scharrer, D., Schmitt, B., Steger, D., German, R., Karellas, S., Pruckner, M., Schlücker, E., Will, S. & Karl, J. (2018), Reversible heat pump-organic rankine cycle systems for the storage of renewable electricity. *Energies, 11*, 11061352.

Steger, D., Karl, J. & Schlücker, E. (2021). Launch and first experimental results of a reversible heat pump-ORC pilot plant as Carnot battery. In Wieland, C., Karellas, S., Quolin, S., Schifflechner, C., Dawo, F. & Spliethoff, H. (Eds.) *Proceedings of the 6th International Seminar on ORC Power Systems, Munich, Germany* (ID 44, 1-9). Munich, Germany: Technical University of Munich.

Steinmann, W.D. (2014). The CHEST (Compressed Heat Energy STorage) concept for facility scale thermomechanical energy storage. *Energy 69,* 543-552.